MIMO synthetic aperture sonar: Benefits and limitations

Roy Edgar Hansen[1,2,✉]
[1]Norwegian Defence Research Establishment (FFI), Kjeller, Norway
[2]Department of Informatics, University of Oslo, Oslo, Norway
✉Email: roy-edgar.hansen@ffi.no

The use of Multiple Input Multiple Output (MIMO) orthogonally coded waveforms sharing the same bandwidth, has the potential to increase area coverage rate in synthetic aperture sonar (SAS). The disadvantage is cross-talk between the waveforms. In this letter, the benefits and limitations are listed for a best case use of MIMO in SAS. A scheme is developed to emulate a MIMO system with realistic cross-talk that can be tested on non-MIMO SAS data. The impact of cross-talk is evaluated on simulated data and real data collected by a HISAS interfereometric SAS carried by a HUGIN autonomous underwater vehicle. The finding is that the negative impact of cross-talk on SAS is significant.

Introduction: Synthetic aperture sonar (SAS) technology has matured substantially since its invention more that 50 years ago [1]. From the very beginning, it has been clear that the sampling requirement along-track imposes a limitation to the area coverage rate [2]. The standard technique in SAS is to use N independent receiver elements placed along-track, thereby gaining an N-fold increase in the area coverage rate. To our knowledge, all commercial systems use this technique today. There are, however, disadvantages related to the multi-element receiver design such as increased hardware complexity and physical size.

Multiple Input Multiple Output (MIMO) orthogonally coded waveforms sharing the same bandwidth is an attractive alternative that has gained massive popularity in radar [3] and in Synthetic Aperture Radar (SAR) [4]. MIMO has also been suggested in sonar [5, 6], and in SAS [7–9]. In the latter case, the disadvantages are not fully described.

In this letter, we consider a setup for doubling the area coverage rate using MIMO in SAS for imaging and mapping the seabed using two orthogonal coded waveforms, known as *Code Division Multiplexing* (CDM) [10, chapter 4.5]. The disadvantage is cross-talk. Following [11], we consider how this cross-talk manifests itself in SAS imaging and SAS interferometry. We emulate a MIMO SAS system by using real data from a non-MIMO SAS system, the HISAS interferometric SAS carried by a HUGIN autonomous underwater vehicle (AUV) [12]. We illustrate the effect of cross-talk on the various SAS data products. Our findings are that MIMO SAS may be used in sparse scenes with strong targets of interest. The negative effect of cross-talk can then be controlled by choosing a large time-bandwidth product in the transmit waveforms. MIMO SAS does not allow for micronavigation or interferometry processing in speckle scenes. This is a rather fundamental drawback that must be taken into account when considering using MIMO for SAS imaging and mapping of the seabed.

Method: We consider the best case scenario for doubling the area coverage rate using MIMO in SAS for imaging the seabed in a sidelooking geometry. The idea is rather simple. By using the *virtual array* principle [10, chapter 4.3], two transmitters correctly placed relative to each other in combination with a receiver array, will double the number of virtual elements. This is illustrated in Figure 1. The system operates by transmitting two orthogonal waveforms sharing the same bandwidth simultaneously, and decoding both signals at each receiver for each transmit. Thereby, the system can move a distance equal to the length of the receiver array, L, between transmits, instead of the usual $L/2$ dictated by the virtual array principle. The doubling of displacement between transmits then again allows for a doubling of maximum range for fixed platform speed. We will refer to this as MIMO SAS. Normal well sampled SAS will be referred to as *original SAS* or *non-MIMO SAS*.

Various different MIMO waveforms have been studied extensively [13]. In this study, we only consider Linear Frequency Modulated (LFM) upchirp and downchirp [14, chapter 4.6]. More advanced waveforms, such as the OFDM-chirp [15], may be needed when more than two simultaneous transmissions are needed. The up/down-chirp waveform pair is near optimum both regarding imaging performance and cross-talk performance. The peak auto-correlation to peak cross-correlation power ratio (PCCR) between these two waveforms is [6]

$$PCCR \approx \frac{1}{BT}, \tag{1}$$

where B is the signal bandwidth, and T is the pulse length.

There are two main negative effects caused by MIMO in SAS:

1. The cross-correlation between the different waveforms will cause a non-zero component (cross-talk) in the entire time spread of the correlation function, approximately equal to two times the length of the waveform. This is a pure 1D effect.
2. The stacking of virtual elements from each waveform into a synthetic aperture will cause a periodic variation that will cause undesired ghost targets in the image, also referred to as *grating lobes*.

These effects will manifest themselves differently, dependent of the seafloor scene content.

Figure 2 shows a SAS image of a simulated point scatterer using non-MIMO (original mode) (upper) and the corresponding MIMO SAS image (lower). The x-axis is along-track and the y-axis is ground range. The maximum value cross-track and along-track is shown in Figure 3. The blue curve represents the MIMO-case, and the red curve is the original case. Note that the point target is correctly positioned in both cases (the blue curve lies under the red). In this particular case, $BT = 240$.

The dominating differences are the main grating lobe at approximately x = 1.2 m, and the range spread of the cross-talk along the y-axis. We see that the PCCR is slightly higher than 20 dB, which corresponds well with the used waveform time-bandwidth product. Note that the peak

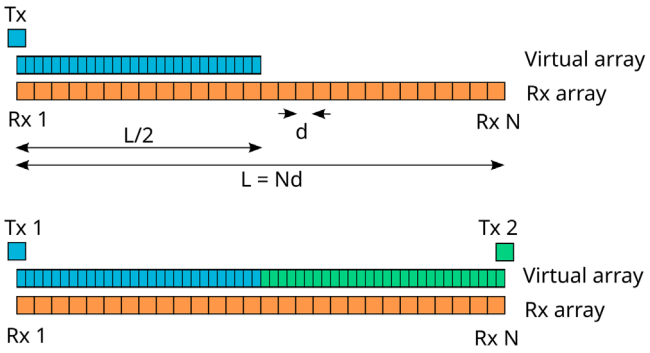

Fig. 1 *Transmitter and receiver element layout. Upper: Standard SAS setup. Lower: Suggested MIMO SAS setup that doubles the virtual array length and thereby doubles the area coverage-rate*

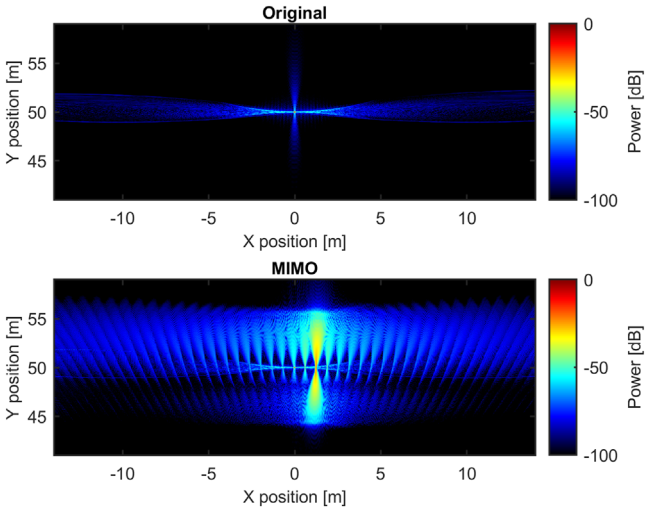

Fig. 2 *SAS image of single point scatterer. Upper: Original SAS image (non-MIMO). Lower: MIMO SAS image*

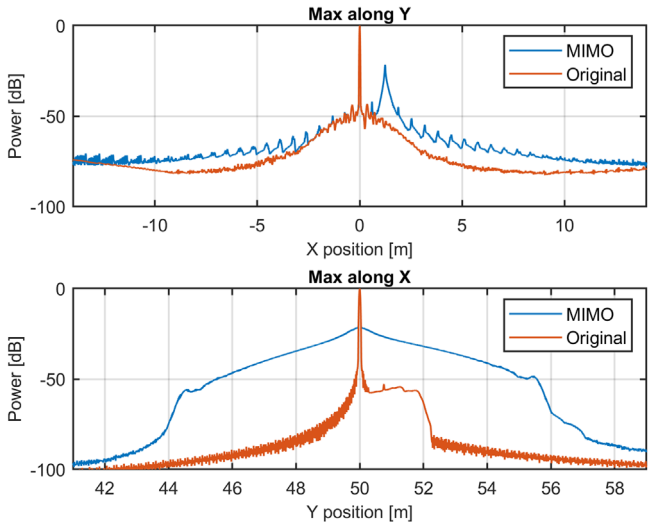

Fig. 3 *Upper: Maximum value cross-track (Y) for the orignal (red) and MIMO (blue) as function of along-track (X) position. Lower: Maximum value along-track (X) for the original (red) and MIMO (blue) as function of cross-track (Y) position*

grating lobe in the upper panel of Figure 3 corresponds to the dominating yellow feature in the lower panel of Figure 2. The grating lobes are placed [16]

$$\Delta x \approx \pm nR\frac{\lambda}{2L_x}, \quad n = 0, 1, 2, \ldots, \tag{2}$$

relative to the main lobe at distance R, where λ is the acoustic wavelength, and L_x is the interval between change in the synthetic aperture. In this paricular case, the center frequency is 100 kHz, giving $\lambda = 1.5$ cm. For a target at $R = 50$ m range, the distance between grating lobes becomes $\Delta x \approx 50 \times 0.015/1.2 \approx 0.6$ m. Note that the second grating lobe is strongest in this case. This is due to how the virtual array was constructed. The range spread from the cross-correlation is approximately equal to

$$\Delta R_{cc} = \pm cT/2, \tag{3}$$

where c is the sound speed. This equals to ± 6 m in our case, where $T = 8$ ms. We see that this corresponds well with the range spread along the y-axis in Figure 3.

A scene containing a single point scatterer represents the ideal textured case. The peak cross-talk can then be controlled by choosing a high enough waveform time-bandwidth product. In the case of a distributed scatterer, cross-talk becomes a more severe issue. Consider a fully developed speckle scene with homogeneous backscatter level. At every sample inside the cross-correlation, an equal amount of undesired cross-talk leaks through, and since there are BT independent samples in the correlation window, the sum of all cross-talk into each sample becomes equal to the signal level per sample. Hence, the signal to cross-talk level becomes 1 (or 0 dB). This follows directly from first principles since the signal energy is independent of waveform and that pulse compression does not change the signal energy [14, chapter 4.2]. It also follows from Parseval's theorem. See [11] for a detailed description of this. The direct consequence of this is that MIMO CDM SAS with two orthogonal waveforms sharing the same bandwidth does not allow for micronavigation [17] or interferometry based on speckle scenes.

To summarize, the negative effects of MIMO in SAS are the dependent of the scene content as follows:

Point scatterer: The signal to peak cross-talk level is approximately $1/BT$ (best case) on the backscattered signal from a single point scatterer.

Speckle: The signal to cross-talk level is 0 dB on the backscattered signal from a speckle scene.

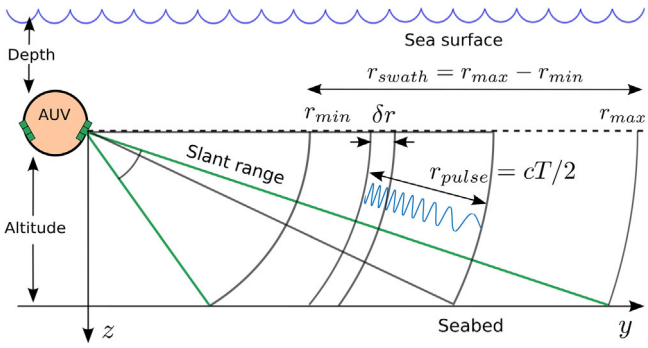

Fig. 4 *Typical vertical geometry for SAS carried by an AUV*

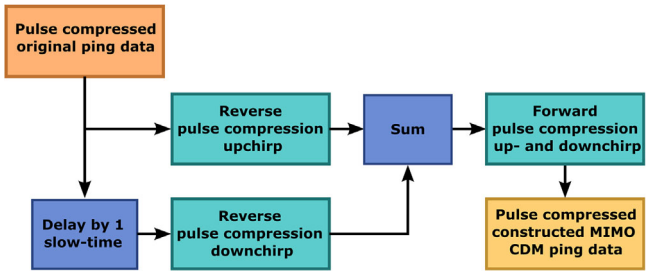

Fig. 5 *Suggested procedure to emulate a MIMO SAS system using original (non-MIMO) data*

Note that the 0 dB cross-talk only applies when using two orthogonal waveforms sharing the same bandwidth. The cross-talk problem is larger when more than two orthogonal waveforms are used simultaneously.

Reducing the negative effect: A technique to reduce the peak grating lobe level in SAR is to use variable Pulse Repetition Frequency (PRF) that effectively reduce the periodicity of the variation in the synthetic aperture [18]. In SAS, variable PRF will inherently either cause gaps in the synthetic aperture, loss of area coverage rate or loss in the micronavigation performance [17]. It will therefore be of limited use.

A proposed solution to the cross-talk problem in distributed scenes is to use so-called *short-term shift-orthogonal* waveforms in addition with cross-track vertical beamforming [11]. This technique is based on moving the main cross-correlation energy outside the observable swath. The cross correlation signal energy is then effectively reduced by beamforming the receiver in the vertical cross-track plane. Thus, this technique reduce the cross-talk both in the point scatter case and in the speckle case. However, in SAS, this approach cannot easily be used, since the range extent of the transmit waveform r_{pulse} always is significantly shorter than the desired imaging swath r_{swath} and longer than the range resolution after pulse compression δr (see Figure 4)

$$r_{swath} \gg r_{pulse} \gg \delta r. \tag{4}$$

Hence, it is virtually impossible to place the cross correlation energy outside the observable swath in a typical SAS imaging geometry. In addition, vertical receive arrays for vertical beamforming adds significant cost and complexity to the system.

Results: In order to judge the suitability of MIMO in SAS, we suggest a procedure to emulate MIMO data from a non-MIMO well sampled data set. The approach is as follows (see Figure 5). We start with the pulse compressed data per pulse. We run reverse pulse compression (or pulse decompression) [19, chapter 1.6] to construct raw upchirp data from ping P and raw downchirp data from ping $P - 1$. We then sum the constructed raw data and run forward pulse compression per waveform as if this was a MIMO system. This will construct an equivalent set of virtual elements containing both waveforms per transmit. The slow-time position of the transmitters will however not be equal to a true MIMO setup as described in Figure 1. Arguably, the cross-talk will be realistic. Therefore, this test is representative regarding the negative

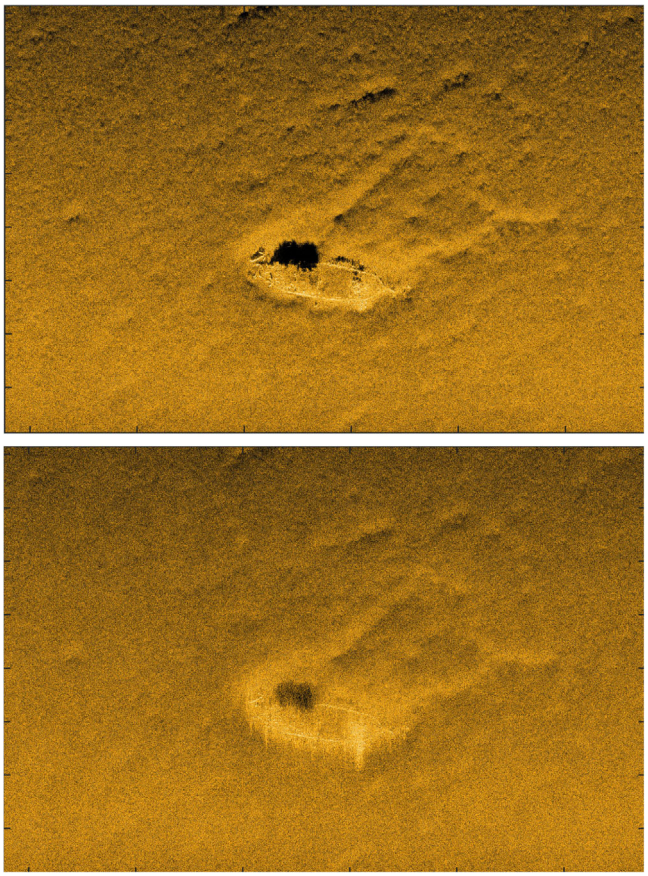

Fig. 6 *SAS image of a small historic shipwreck. The imaging scene is 100 x 80 m. The dynamic range is 40 dB. Upper: Original. Lower: MIMO*

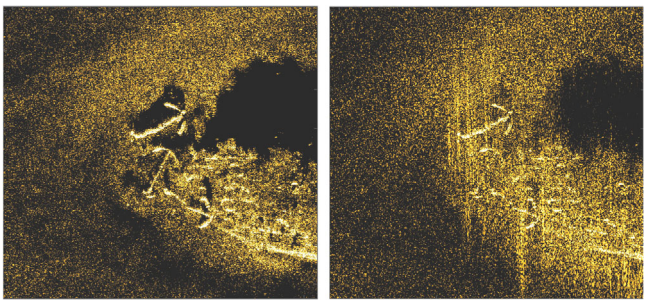

Fig. 7 *17 x 15 m zoom of the bow area of the shipwreck. The dynamic range is 20 dB. Left: Original. Right: MIMO*

consequences of MIMO in SAS. We have tested our approach on real data collected with a HISAS interferometric SAS carried by a HUGIN AUV. The carrier frequency and waveform parameters are the same as for the simulated case in the previous section. It should be noted that we have chosen to use the navigational solution and the geometry solution based on the original data (the non-MIMO data) for the MIMO case. The only effect shown in the following images are from the actual cross-talk in the imaging. There are no extra defocusing or grating lobes from non-working micronavigation or pre-SAS geometry estimation. The images are formed using the backprojection algorithm, and the interferometry processing is done using a cross-correlation technique with a 9×9 pixel window size. See [12, 20] for details on the processing.

Figure 6 shows a SAS image of a small historic shipwreck in the Skagerrak strait. The upper image is the original SAS image, and the lower image is the MIMO SAS image. The shipwreck lies in a benign area of very little texture. We see a loss of contrast, mainly in the range dimension. Figure 7 shows a zoom around the bow area, where we can see three anchors. In the MIMO SAS image we see a clear loss of shadow depth. This is the expected effect of the cross-talk. The highlight features are, however, preserved. Recap that the benefit of MIMO SAS is the doubling of the area coverage-rate.

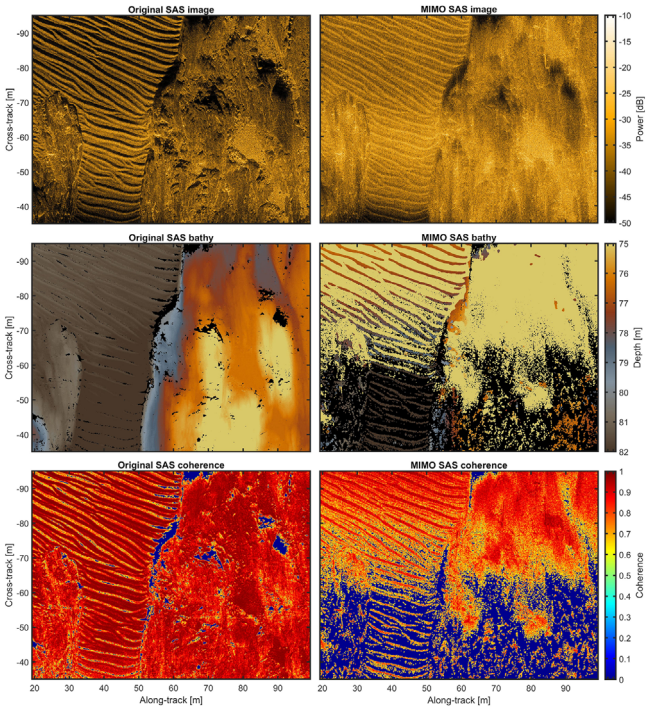

Fig. 8 *Original (left) and MIMO (right) SAS image (upper), SAS bathymetry (middle) and SAS interferometric coherence (lower) of a textured scene with topographic variations. The imaging scene is 80 x 60 m*

Figure 8 shows the SAS image (upper), the bathymetry (middle) and the interferometric coherence (lower) of a heavily textured natural scene with sand ripples, rock outcrops and smooth rock. The left panels show the original data, and the right panels show the MIMO data. The dominating effect of cross-talk in the SAS image is the loss of contrast due to the range spread, and to some degree the grating lobes. At cross-track distances from -35 m to -65 m, the interferometric coherence is significantly lower in the MIMO case. This is caused by the cross-talk extent cross-track and its vertical angular spread. At larger (negative) cross-track, this effect is less pronounced. We see; however, that the depth estimates are essentially incorrect in the entire scene. In this textured case, we therefore conclude that MIMO cannot be used in SAS when interferometry processing is expected to work.

Conclusions: In this letter, we have investigated using two orthogonal waveforms sharing the same bandwidth in a MIMO SAS setup. The benefit of this is a doubling of the area coverage rate with a small impact on the hardware complexity. This is a significant improvement. The main drawback using MIMO in SAS is cross-talk between the waveforms. The cross-talk is impossible to avoid for normal SAS imaging geometries and normal waveforms, as long as the waveforms share the same bandwidth. The impact of the cross-talk on the backscattered signal is dependent on the imaging scene content. For relatively sparse scatterers of high signal value, the cross-talk can be controlled by adjusting waveform bandwidth and pulse length.

For large speckle scenes, the signal and cross-talk level are equal independent of choice of waveform. This is a significant disadvantage that effectively prohibits the use of micronavigation and interferometry on speckle scenes. We have developed a methodology for emulating a MIMO SAS system based on data from a normal (non-MIMO) SAS. We have illustrated the effect of cross-talk on simulated data and real data from a HISAS interferometric SAS carried by a HUGIN AUV, both on a small high contrast target and on a heavily textured scene. We show that the interferometry processing totally fails in the textured case.

Author contributions: Roy Edgar Hansen: Conceptualization, data curation, formal analysis, investigation, methodology, resources, software, validation, visualization, writing - original draft, writing - review and editing.

Acknowledgements: The author acknowledge Dr. Gerhard Krieger at the German Aerospace Center (DLR), Germany, and Dr. Antoine Blachet, formerly at University of Oslo, Norway, now at Thales Underwater Systems, France, for valuable discussions. The author also thanks the SAS-team at FFI, and the colleagues at University of Oslo.

Conflict of interest: The authors have declared no conflict of interest.

Data availability statement: Research data are not shared.

Received: *11 November 2022* Accepted: *23 December 2022*
doi: 10.1049/ell2.12723

References

1 Sternlicht, D.D., Hayes, M.P., Hansen, R.E.: Seabed mapping sas: The first 50 years of synthetic aperture sonar imaging technology. *Sea Technol. Mag.* **59**(11), 10–14 (2018)
2 Hayes, M.P., Gough, P.T.: Synthetic aperture sonar: A review of current status. *IEEE J. Oceanic Eng.* **34**(3), 207–224 (2009)
3 Li, J., Stoica, P.: *MIMO Radar Signal Processing*. Wiley, Hoboken, NJ (2009)
4 Wang, W.Q.: MIMO SAR imaging: Potential and challenges. *IEEE Aerosp. Electron. Syst. Mag.* **28**(8), 18–23 (2013)
5 Pailhas, Y., Petillot, Y., Brown, K., Mulgrew, B.: Spatially distributed MIMO sonar systems: Principles and capabilities. *IEEE J. Oceanic Eng.* **42**(3), 738–751 (2017)
6 Blachet, A., Austeng, A., Aparicio, J., Hunter, A.J., Hansen, R.E.: Multibeam echosounder with orthogonal waveforms: Feasibility and potential benefits. *IEEE J. Oceanic Eng.* **46**(3), 963–978 (2021)
7 Qiao, Z., Buß, M., Zimmer, C., Kraus, D., Zoubir, A.M.: Investigation on point spread function of MIMO SAS with frequency modulated waveforms. In: Proceedings of the OCEANS 2018 MTS/IEEE. Charleston, SC, USA (2018)
8 Kerstens, R., Laurijssen, D., Steckel, J.: An optimized planar MIMO array approach to in-air synthetic aperture sonar. *IEEE Sens. Lett.* **3**(11), 1–4 (2019)
9 Xenaki, A., Pailhas, Y., Sabatini, R.: Sparse MIMO synthetic aperture sonar processing with distributed optimization. In: Proceedings of the 54th Asilomar Conference on Signals, Systems, and Computers. IEEE, Piscataway (2020)
10 Melvin, W.L., Scheer, J.A.: *Principles of Modern Radar. Vol II: Advanced Techniques*. Scitech Publishing, Edison, NJ (2013)
11 Krieger, G.: MIMO-SAR: Opportunities and pitfalls. *IEEE Trans. Geosci. Remote Sensing* **52**(5), 2628–2645 (2014)
12 Hansen, R.E., Callow, H.J., Sæbø, T.O., Synnes, S.A.V.: Challenges in seafloor imaging and mapping with synthetic aperture sonar. *IEEE Trans. Geosci. Remote Sensing* **49**(10), 3677–3687 (2011)
13 García, E., Paredes, J.A., Álvarez, F.J., Pérez, M.C., García, J.J.: Spreading sequences in active sensing: A review. *Signal Process.* **106**, 88–105 (2015)
14 Richards, M.A.: *Fundamentals of Radar Signal Processing*, 2nd ed. Mcgraw-Hill Book Company, New York (2014)
15 Wang, W.Q.: MIMO SAR OFDM chirp waveform diversity design with random matrix modulations. *IEEE Trans. Geosci. Remote Sensing* **53**(3), 1615–1625 (2015)
16 Cook, D.A., Brown, D.C.: Analysis of phase error effects on stripmap SAS. *IEEE J. Oceanic Eng.* **34**(3), 250–261 (2009)
17 Bellettini, A., Pinto, M.A.: Theoretical accuracy of synthetic aperture sonar micronavigation using a displaced phase-center antenna. *IEEE J. Oceanic Eng.* **27**(4), 780–789 (2002)
18 Villano, M., Krieger, G., Moreira, A.: Staggered SAR: High-resolution wide-swath imaging by continuous PRI variation. *IEEE Trans. Geosci. Remote Sensing* **52**(7), 4462–4479 (2014)
19 Soumekh, M.: *Synthetic Aperture Radar Signal Processing*. Wiley-Interscience, New York (1999)
20 Sæbø, T.O., Synnes, S.A.V., Hansen, R.E.: Wideband interferometry in synthetic aperture sonar. *IEEE Trans. Geosci. Remote Sensing* **51**(8), 4450–4459 (2013)